

Assessing the perturbations of the hydrogeological regime in sloping fens through roads

Fabien Cochand¹, Daniel Käser¹, Philippe Grosvernier², Daniel Hunkeler¹, Philip Brunner¹

¹Centre of Hydrogeology and Geothermics, Université de Neuchâtel, Switzerland.

²LIN'eco, ecological engineering, PO Box 51, 2732 Reconvilier, Switzerland.

Corresponding author: Fabien Cochand, fabien.cochand@unine.ch

Abstract

Roads in sloping fens constitute a hydraulic barrier for surface and subsurface flow. This can lead to the drying out of downslope areas of the sloping fen as well as gully erosion. Different types of road construction have been proposed to limit the negative implications of the roads on flow dynamics. However, so far no systematic analysis of their effectiveness has been carried out. This study presents an assessment of the hydrogeological impact of three types of road structures in semi-alpine, sloping fens in Switzerland. Our analysis is based on a combination of field measurements and fully integrated, physically based modelling. In the field approach, the influence of the road was examined through tracer tests where the upslope of the road was sprinkled with a saline solution. The spatial distribution of electrical conductivity downslope provided a qualitative assessment of the flow paths and thus the implications of the road structures on subsurface flow. A quantitative albeit not site-specific assessment was carried out using numerical models simulating surface and subsurface flow in a fully coupled way. The different road types were implemented in the model and flow dynamics were simulated for a wide range of slopes and hydrogeological conditions such as different hydraulic conductivity of the soil. The results of the field and modelling analysis are coherent. Roads designed with an L-drain collecting water upslope and releasing it in a concentrated manner downslope constitute the largest perturbations. The other investigated road structures were found to have less impact. The developed methodologies and results are useful for the planning of future road projects.

1 **1 Introduction**

2 Wetlands can play a significant role in flood control (Baker, 2009;Zollner, 2003;Reckendorfer, 2013),
3 mitigate climate change impacts (Cognard Plancq et al., 2004;Samaritani et al., 2011;Lindsay, 2010;Limpens,
4 2008) and feature great biodiversity (Rydin, 2005). However, the world has lost 64% of its wetland areas since
5 1900 and an even greater loss has been observed in Switzerland (Broggi, 1990). Therefore, wetland conservation
6 has received considerable attention. However, the sprawl of human infrastructure, land use changes, climate
7 change or river regulations remain serious factors that threaten wetlands. For instance, roads can substantially
8 modify the surface-subsurface flow patterns of sloping fens. The changes in flow patterns can influence sediment
9 transport, moisture dynamics and biogeochemical processes as well as ecological dynamics.

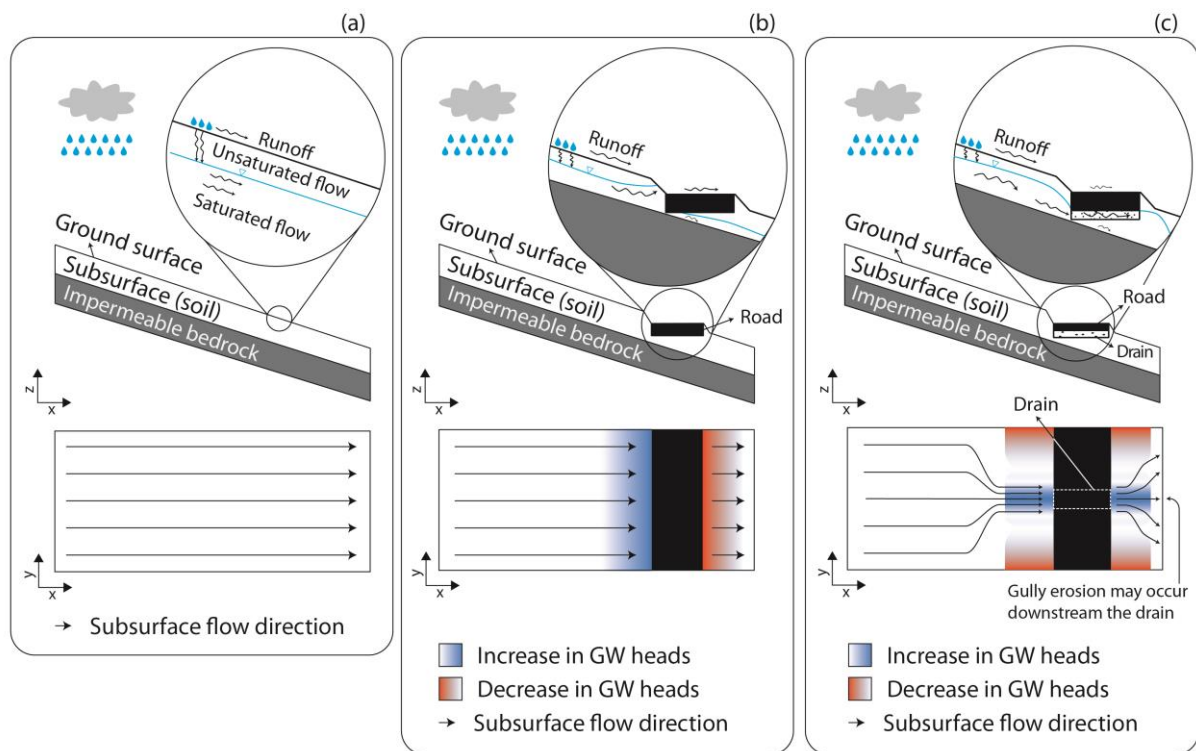
10 The link between hydrological changes and sediment dynamics has been studied in various contexts.
11 From a civil engineering perspective, erosion of the road must be avoided. A common strategy to avoid erosion
12 of the road foundation is to collect water in drains and then release it in a concentrated manner downslope. This,
13 however, can lead to erosion of the downslope area, a phenomenon known as « gully erosion ». A number of
14 studies specifically focused on identifying the controlling processes and relevant parameters of gully erosion
15 (Capra et al. (2009);Valentin et al. (2005a);Descroix et al. (2008);Poesen et al. (2003);Martínez-Casasnovas
16 (2003);Daba et al. (2003);Betts and DeRose (1999);Derose et al. (1998), among others). Nyssen et al. (2002)
17 investigated the impact of road construction on gully erosion in the northern Ethiopian highlands, with a focus
18 on surface water. In their study area, they observed the formation of a gully after the road construction
19 downslope culvert and outlets of lateral road drains. Based on fieldwork and a subsequent statistical analysis,
20 they concluded that the main causes for gully development are the concentrated runoff, the diversion of
21 concentrated runoff to other catchments and the modifications of drainage areas induced by the road. The role of
22 groundwater was not considered in this study.

23 Reid and Dunne (1984) developed an empirical model for estimating road sediment erosion of roads
24 located in forested catchments in the Washington state (USA). They concluded that a heavily used road produced
25 130 times more sediment than an abandoned road. Wemple and Jones (2003) also developed an empirical model
26 for estimating runoff production of a forest road at a catchment scale. They demonstrated that during large storm
27 events, subsurface flow can be intercepted by the road. The intercepted water, if directly routed to ditches,
28 increases the rising limb of the catchment hydrograph. At a smaller spatial scale (0.1 km²) Loague and
29 VanderKwaak (2002) assessed the impact of a road on the surface and subsurface flow using an integrated

30 surface-subsurface flow model InHM (Integrated Hydrology Model) (VanderKwaak, 1999) in a rural catchment.
31 The results showed that the road induced a slight increase of runoff and a decrease of surface-subsurface water
32 exchange around the road. Dutton et al. (2005) investigated the impact of roads on the near-surface subsurface
33 flow using a variability saturated subsurface model. They concluded that the permeability contrast caused by the
34 road construction leads to a disturbance of near-surface subsurface flow which may significantly modify the
35 physical and ecological environment.

36 Road construction can also impact the development of vegetation (Chimner, 2016). Von Sengbusch
37 (2015) investigated the changes in growth of bog pines located in a mountain mire in the black forest (south-west
38 Germany). The author suggests that the increase of bog pine cover is caused by a delayed effect of a road
39 construction in 1983 along a margin of the bog. The road affects subsurface flow and therefore prevents the
40 upslope water to flow to the bog. According to von Sengbusch (2015), the road disturbances induce a larger
41 variability in water table elevations during dry periods and consequently increase the sensitivity of the bog to
42 climate change.

43 Based on these previous studies and basic principles of subsurface flow, a simple conceptual model
44 describing the influence of roads on the flow system can be drawn (Figure 1). Roads are generally built with
45 materials of low hydraulic conductive and therefore constitute a hydrogeological barrier. In natural conditions,
46 rainwater infiltrates the soil and follows the topographical gradient. In case of heavy precipitation events, water
47 can also directly flow on the surface (Figure 1a) as overlandflow. If a road is constructed, it constitutes a
48 hydrogeological barrier (Figure 1b) and consequently affects the flow dynamics. Drains installed underneath the
49 road (Figure 1c) can mitigate the effect of this hydrogeological barrier. The design and the materials of drains
50 significantly affect flow dynamics. Figure 1c presents a typical condition where a non-continuous drain (i.e.,
51 drains are perpendicularly installed at regular distances along the road) is used to connect both sides of the road.
52 Upstream and downstream subsurface flows are deviated and the drain becomes the main outlet. The
53 concentration of subsurface flow downstream of the drain may induce gully erosion and disturb the hydraulic
54 regime of the sloping fens.



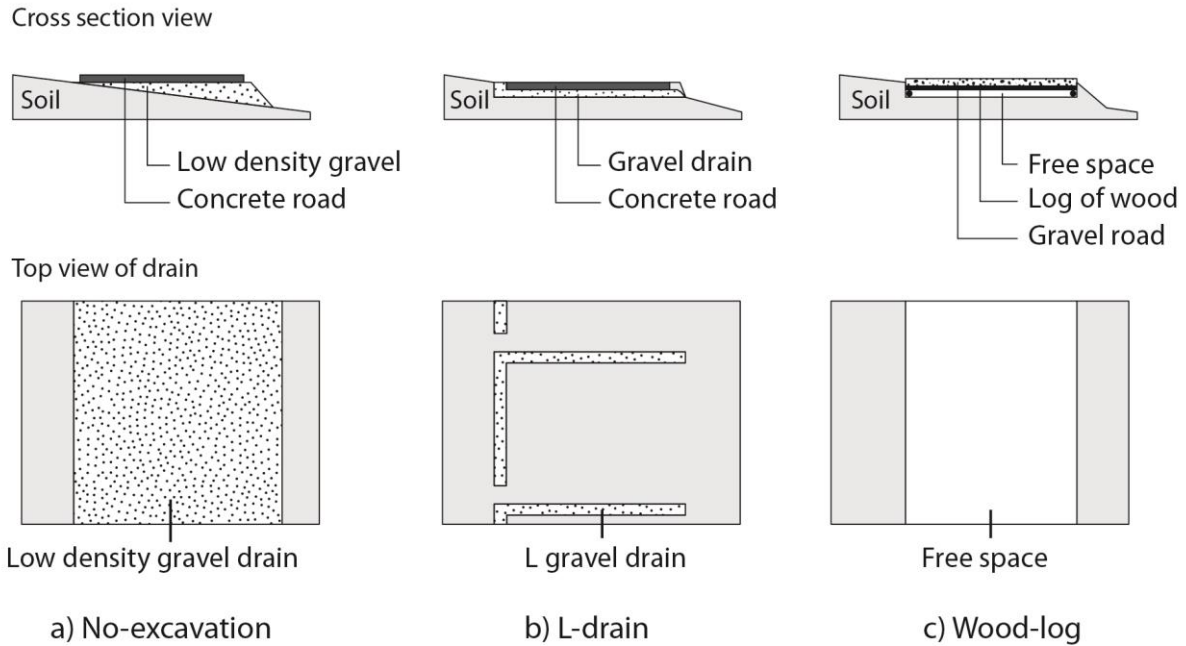
55

56 **Figure 1 Conceptual subsurface dynamics in sloping fens: a) natural conditions, b) with road without a drain and c)**
 57 **with a road and a drain.**

58 While these studies clearly indicate that roads can have adverse effects on the surface and subsurface flow
 59 dynamics and the associated ecosystems, a detailed study on how roads perturb the flow system and dynamics in
 60 a sloping fen has not been carried out. In Switzerland, more than 20'000 ha are included in the national inventory
 61 of fens of national importance (Broggi 1990), most of them are located in the mountainous regions of the
 62 northern Prealps. Hence, the majority of Swiss fens is composed of sloping fens, which developed on nearly
 63 impermeable geomorphological layers such as silty moraine material or a particular rock layer named "flysch".
 64 Although organic, soils are not necessarily peaty and most of the time quite superficial, not exceeding a few
 65 decimeters in thickness. Water flow is therefore mostly consisting of runoff and partly occurring in the shallow
 66 part of the subsurface. The construction of a road in this kind of sloping fens removes completely the soil layer
 67 in which subsurface flow occurs, thus constituting a major perturbation of the hydraulic regime. Construction
 68 techniques to limit these adverse impacts have been proposed but their efficiency has so far not been investigated
 69 Three road structures with various construction techniques and materials (hereinafter further detailed) were
 70 developed in Switzerland to reduce the impacts of roads. These three road types are conceptually illustrated in
 71 Figure 2. The efficiency of developed road structures was so far not assessed after completion, , neither in the
 72 field through field-based experiments, nor on a conceptual level.. This study focuses on these three road
 73 structures described hereafter:

- 74 • The *no-excavation* structure (Figure 2a) aims at preserving soil continuity under the road. It consists of
75 a levelled layer of gravel, anchored to the ground, and underlying 0.16m thick concrete slabs. Soil
76 compaction is limited by using a low-density gravel, made of expanded glass chunks (Misapor™) -
77 approximately fivefold lighter than conventional material.
- 78 • The *L-drain* structure (Figure 2b) aims at collecting subsurface water upstream the road and redirecting
79 it to discrete outlets on the other side. The setup consists of a trench, approximately 0.4m deep, filled
80 with a matrix of sandy gravel that contains an L-shaped band of coarse gravel acting as the drain.
- 81 • The *wood-log* structure (Figure 2c) aims at promoting homogeneous flow under the road but does not
82 preserve soil continuity. Embedded in a trench, approximately 0.4m deep, the wooden framework is
83 filled with wooden logs forming a permeable medium. The wooden logs are then covered with mixed
84 gravel.

85 The aim of this study is to investigate, document and assess the hydrogeological impact of various road
86 structures and their effects on fen water dynamics. A combination of fieldwork and hydrogeological modelling
87 tasks was employed. Fieldwork was used to document and obtain the required information on the
88 hydrogeological impact of existing road structures on fen water dynamics. It is the first time that these road-
89 types are systematically analysed under field conditions and thus provide important information on their
90 effectiveness. Sites with similar natural conditions were chosen to compare the influence of different road
91 constructions on flow processes. The field studies allow for assessing the effectiveness of a given road structure,
92 however, they cannot provide generalizable analysis of the different road types under different environmental
93 and physical conditions, e.g. the slope or the hydraulic properties of the fen. This gap was filled by the
94 development of generic numerical models. The main advantage of the modelling approach is the possibility to
95 generate a multitude of different models with various characteristics such as different road structures, slopes or
96 fen hydraulic conductivity and to test their impacts on the flow dynamics. These model results can help in the
97 planning of new roads.



98

99 **Figure 2 : Conceptual road structures, a) No-excavation road structure, b) L-drain road structure and c)**
 100 **Wood-log road structure.**

101 **2 Methods**

102 **2.1 Study areas and fieldwork**

103 Four sloping fen areas located in alpine or peri-alpine regions of Switzerland (Table 1) were selected. All
 104 areas are situated in protected fen areas, and their selection was based on two main criteria:

- 105 1. The subsurface water flow must occur only in the topsoil layer and as runoff (as described in the
 106 introduction).
- 107 2. The types of installed road structures (no-excavation, L-drain and wood-log).

108 To fulfil the first criteria, soil profiles were analysed to ensure that each area with different road types had the
 109 comparable soil stratigraphy: It had to be composed of organic soil on top of a layer of impermeable clay and
 110 similar hydraulic regimes (e.g., runoff and subsurface flow occurring only in the topsoil layer). In addition, to
 111 ensure that subsurface water is forced to cross the road instead of flowing in parallel of the road (and thus not
 112 being affected directly by the road), another important criterion for the selection of the study areas was that
 113 subsurface flow is perpendicular to the road.

114 To evaluate the hydraulic connection provided by the roadbed structures, tracer tests were carried out. As
 115 illustrated schematically in Figure 3, the upslope area was irrigated with a saline solution and the occurrence of

116 the tracer was monitored downslope the road. In the absence of surface runoff, the occurrence of a tracer
 117 downslope demonstrates the hydrogeological connection through the road. Furthermore, the spatial distribution
 118 of the tracer front reflects the heterogeneity of the flow paths.

119 **Table 1. Field site locations and features.**

| | St-Antonien (STA) | Schoeniseischwand (SCH) | Stouffe (STO) | Hömad (HMD) |
|--------------------------|------------------------------|------------------------------------|-------------------------|-------------------------|
| <i>Road type</i> | No excavation | L-Drain | Wood-log | Wood-log |
| <i>Terrain slope</i> | 0.27 | 0.13 | 0.13 | 0.15 |
| <i>WGS84 coordinates</i> | 46.96760°N 9.84843°E | 46.78872°N 7.96805°E | 46.72957°N 7.83861°E | 46.74027°N 7.89871°E |

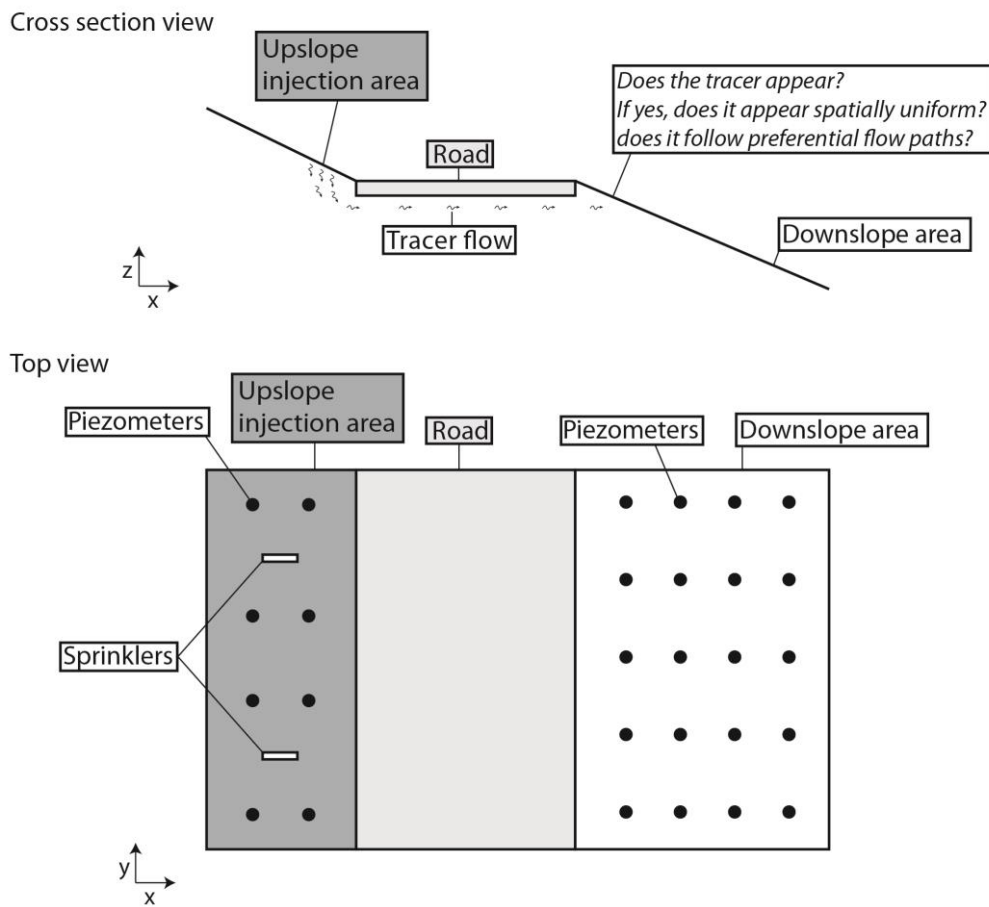
120

121 Each area corresponds to an 8 x 20m rectangle that includes a 2.5 to 3.5m wide road segment. A network
 122 of approximately 30 mini-piezometers on both sides of the road (Figure 3) was installed to monitor the hydraulic
 123 heads and was used to obtain samples for the tracer test.

124 The mini-piezometers are high-density polyethylene (HDPE) tubes no longer than 1.5m (ID: 24mm). Each
 125 tube was screened with 0.4mm slots from the bottom end to 5cm below ground level. It was inserted into the soil
 126 after extracting a core with a manual auger (diameter: 4-6cm). The gap between the tube and the soil was filled
 127 with fine gravel and sealed on the top with a 4cm thick layer of bentonite or local clay. Hydraulic heads were
 128 measured using a manual water-level meter (± 0.3 cm). At each point, the terrain and the top of the piezometer
 129 were levelled using a level (± 0.3 cm), whereas the horizontal position was measured with a tape measure (\pm
 130 5cm).

131 The tracer tests were conducted using two oscillating sprinklers designed to reproduce a 30mm rain event
 132 during 2-3 hours. This is equivalent to an intense rain event. Prior to the experiment, the sprinklers were
 133 activated for 15-60 minutes to wet the soil surface. Sodium chloride was added to the irrigated solution to obtain
 134 an electrical conductivity of 5-10mS/cm which is approximately ten times higher than the natural electrical
 135 conductivity of the groundwater. Then, the area (60m²) upslope of the road (upslope injection area of Figure 3)
 136 was irrigated with the salt solution using the two sprinklers. The electrical conductivity (EC) of soil water was
 137 manually measured using a conductivity meter in all mini-piezometers prior to the experiment, immediately
 138 after, and 24h later. An increase in EC in piezometers located in the downslope area indicates that the injected
 139 salt water flowed from the upslope area to the downslope area below the road and clearly shows a hydraulic

140 connection. Conversely, if no changes in EC are observed in piezometers, this indicates a strongly hampered
141 hydraulic connection below the road.



142
143 **Figure 3 : Schematic view of the fieldwork areas.**

144 **2.2 Numerical modelling**

145 To quantify the impact of the roads on the flow dynamics in sloping fens in a generalized way, the
146 modelling approach was structured in three steps. First, a 3D base case model representing surface and
147 subsurface water flow in a sloping fen was elaborated. Subsequently, the base case model was modified to
148 represent the three different types of investigated road structures. For each model, various slopes, organic soil
149 and road drain hydraulic conductivities were implemented to produce a sensitivity analysis and explore their
150 sensitivities in the sloping fen flow dynamics (see section 2.2.3 for details). Finally, a comparison of all model
151 results was made in order to assess the impact of road structures and quantify the dynamics and the physical
152 controls of subsurface flow in these environments. These controls include the slope of the fen and the hydraulic
153 properties of the subsurface material.

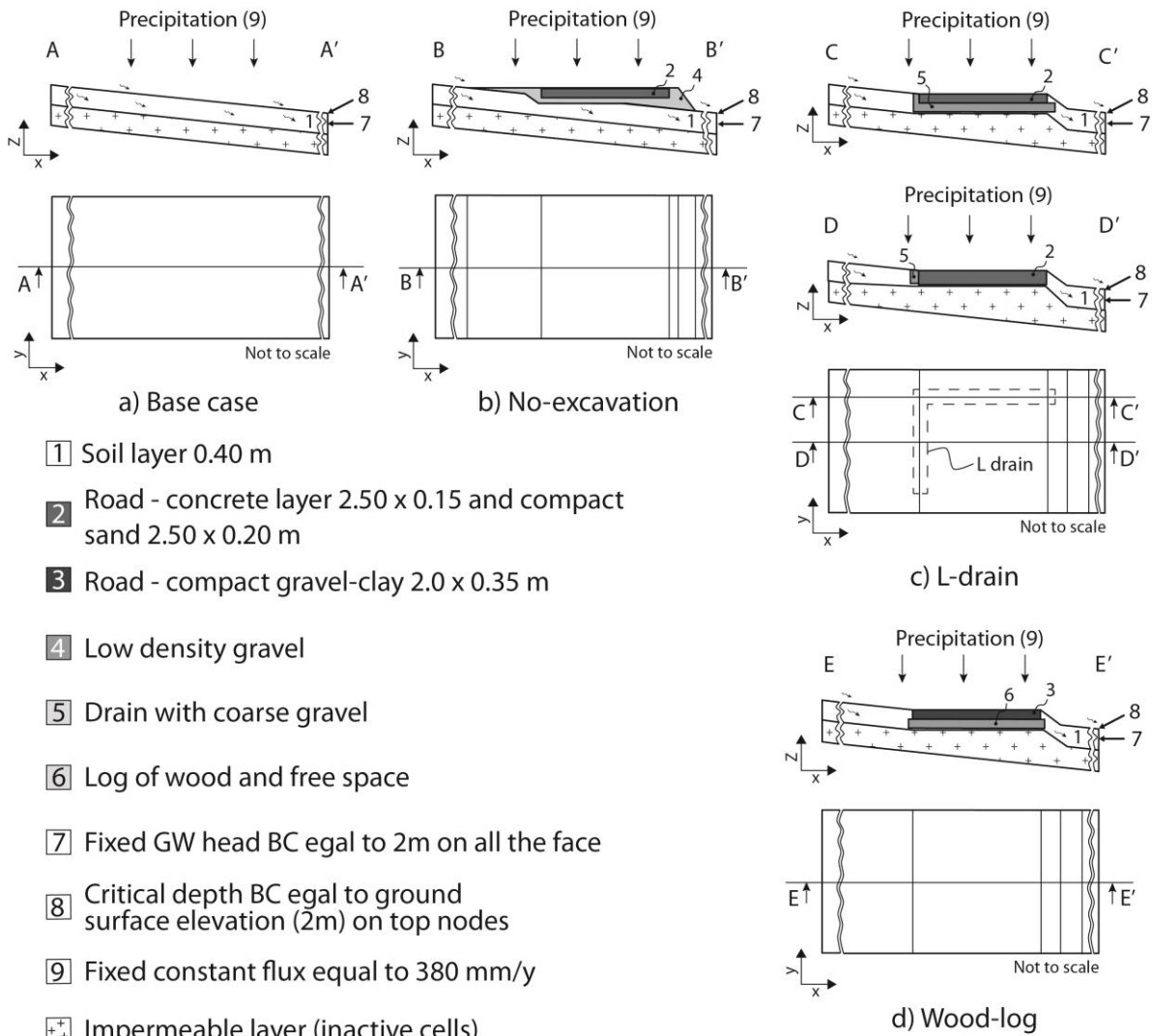
154 **2.2.1 Numerical simulator**

155 The model used in the study is HydroGeoSphere (HGS) (Aquanty, 2017). HGS is a physically-based surface–
156 subsurface fully-integrated model using the control volume finite element approach. HGS solves a modified
157 Richards’ equation describing the 3D subsurface flow. If the subsurface flow is not saturated, HGS employs the
158 Van Genuchten (1980) functions to relate pressure head to saturation and relative hydraulic conductivity.
159 Simultaneously, HGS also solves the 2D depth average diffusion-wave approximation of the Saint-Venant
160 equation for describing the surface flow. To couple surface and subsurface and simulate the water exchanges
161 between both domains, the “dual node approach” is used. In this approach, the top nodes representing the ground
162 surface are used for calculating both subsurface and surface flow. The water exchanges are calculated as
163 hydraulic head differences of the two domains and multiplied by the vertical hydraulic conductivity of the top
164 layer and a coupling factor.

165 The iterative Newton-Raphson method is used to solve the nonlinear equations. At each subsurface node,
166 saturation and groundwater heads are calculated, which allows for the calculation of the Darcy flux. On the
167 surface domain, the surface water heights are calculated at each node to determine surface water flux. Rivers and
168 lakes are characterized by a surface water depth larger than 0. For further details on the code, HGS capabilities
169 and application, see Aquanty (2017), Brunner and Simmons (2012) or Cochand et al. (2019).

170 **2.2.2 Conceptual models and model implementation**

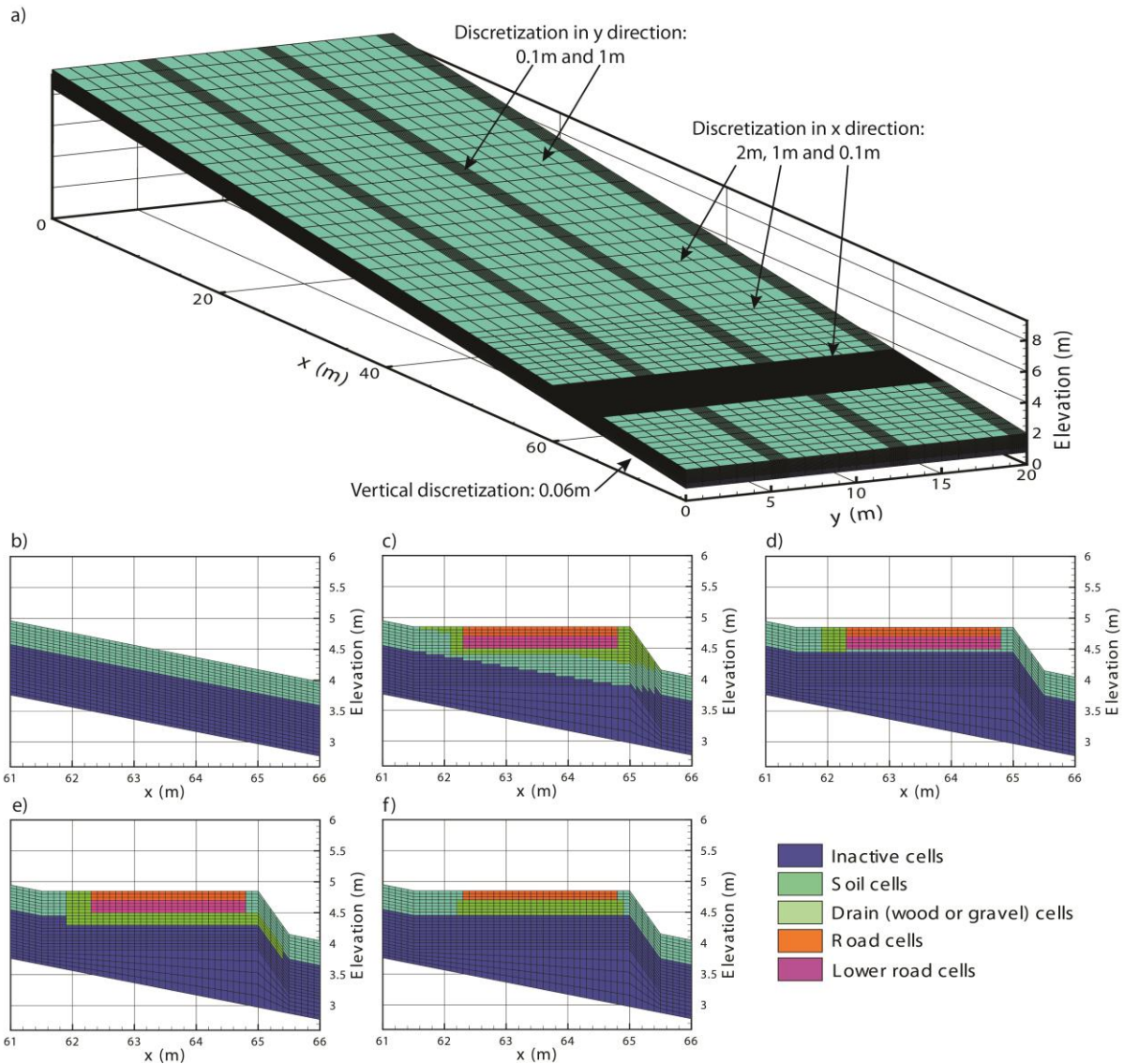
171 Figure 4 illustrates the conceptual model of each case. Geometry, topography, and slopes are based on the
172 physical conditions in the field. In each model, the soil layer has a thickness of 0.4m and the surface and
173 subsurface water are only supplied by precipitation. The upstream boundary is the catchment boundary (water
174 divide) and the downstream boundary represents the outlet of the model. Finally, it was assumed that the layer
175 beneath the soil was impermeable (as observed in the field) and engineering plans were used to design drain and
176 road. One Neumann (constant flux) boundary condition was used on the top face for simulating precipitation. A
177 constant groundwater head boundary condition (Dirichlet type) equal to the ground surface elevation (2m) was
178 used on the lowest cells of the slope ($x=76\text{m}$ on the Figure 5a) allowing the groundwater to flow out of the
179 model. Finally, a critical depth boundary condition which forces the surface water to reach a given elevation (2m
180 in our case) to flow out of the model was implemented on the top nodes located at $x=76\text{m}$ and all other faces are
181 no flow boundary conditions.



To numerically solve the 3D flow equation, a 3D mesh was developed (Figure 5a). The mesh is 76m long in the X direction, 20m in the Y direction and the mesh thickness is 1.2m. The top elevation was fixed at 2m on the right side ($x=76m$) and varies from 9.6m to 24.8m on the left side ($x=0$) according to the slope of the model. The mesh was made up of 24 layers, 127,200 nodes and 118,440 rectangular prism elements. To ensure an appropriate level of detail, several mesh discretization refinements were made. Therefore, the element size varies between 2m and 0.1m horizontally (in the X and Y directions) and 0.09m and 0.06m vertically.

The base case model and the three other models representing different road types have the same boundary conditions and finite element meshes, however, modifications were made between coordinates $61 < x < 66$ to implement the different road types. Figure 5 depicts the differences between the base case model (Figure 5a and b) and models with roads (Figure 5c, d, e and f). In the case of models with a road, the mesh was deformed and

194 the properties were changed. The fine spatial discretization of the mesh created between the coordinates
 195 $61 < x < 66$ allows a more accurate representation of the simulated processes where high hydraulic gradients are
 196 expected (near roads and drains). Additionally, the refinements allow an accurate representation of drains and the
 197 roads.



198

199 **Figure 5 : Model development: a) Base case model, b) Base case model cross-section between $61m < x < 66m$, c) No-**
 200 **excavation model between $61m < x < 66m$, d) L-drain model between $61m < x < 66m$, e) L-drain model between $61m <$**
 201 **$x < 66m$ along the transversal drain f) Wood-log model between $61m < x < 66m$.**

202 2.2.3 Model setup

203 The sensitivity analysis consists of the variation of model properties and parameters in order to
 204 understand how they control the sloping fen dynamics. The sensitivities of the following parameters were
 205 analyzed: fen slope, soil hydraulic conductivities and road drain hydraulic conductivities. These parameters were

206 selected because they govern the Darcy law (1) and consequently the groundwater dynamics. K is the hydraulic
 207 conductivity of the soil and the drain and ∇H the gradient of the fens controlled by the slope.

$$q = K * \nabla H \quad (1)$$

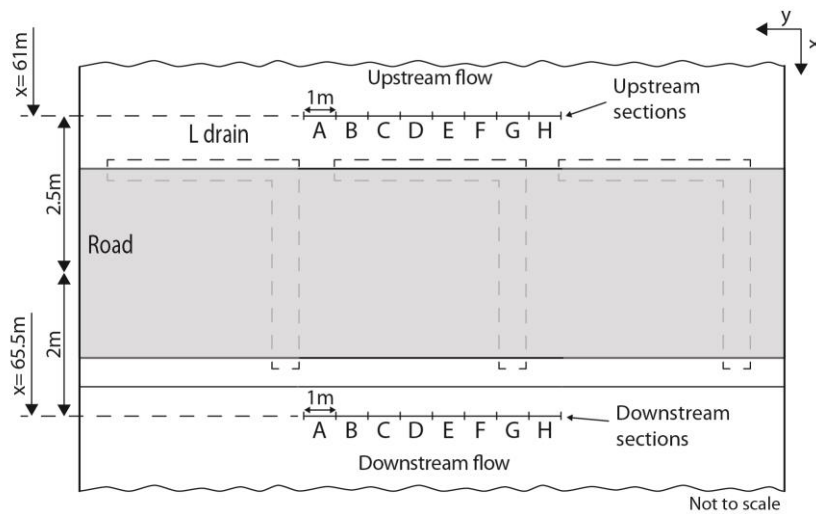
208 For each property, three different values were chosen (Table 2), a low, an intermediate and a high values
 209 with the aim of covering the whole range of its observed values in sloping fens. For the soil hydraulic
 210 conductivities (K_S), values presented in Charman (2002) were used and vary between 8.64m/d and 0.0864m/d.
 211 This corresponds to a soil composed of gravely organic matter (as observed for example in St-Antonien site) or
 212 loamy organic matter (as observed for example in Schoeniseischwand site). α and β Van Genuchten parameters
 213 and the residual water content were considered similar assuming their capillary rises are comparable and does
 214 not play a critical role in a 40cm soil layer mainly saturated. The road drains (KD) which are made with coarse
 215 or very coarse gravel and have a hydraulic conductivity varying between 8640m/d and 86.4m/d (Fetter 2001) and
 216 their van Genuchten parameters are those of gravel. The slopes were fixed at 10%, 20% and 30% as observed
 217 during the fieldwork. Note that the drain hydraulic conductivities of the wood-log (W-L) were assumed ten times
 218 more conductive and more porous than gravel drain because of its particular structure (wood logs). The road
 219 concrete is almost impermeable with a very low hydraulic conductivity and its van Genuchten parameters of fine
 220 material. The road basement made with highly compacted fine material (sand and loam) feature a low hydraulic
 221 conductivity and are assigned van Genuchten parameters corresponding to fine material. Finally, the
 222 implemented soil and road surface flow properties correspond to a wetland and urban cover (Li et al., 2008).

223 *Table 2 : Subsurface and surface flow parameters.*

| Subsurface flow properties | | | | | | |
|----------------------------|------------------------|--------------|------------------------|-----------------------|------------------------|--|
| | Hydraulic conductivity | Porosity | Van Genuchten α | Van Genuchten β | Residual water content | |
| Units | $K [md^{-1}]$ | $\theta [-]$ | $\alpha [m^{-1}]$ | $\beta [-]$ | Swr [-] | |
| Soil - KS1 | 8.64 | 0.25 | 4 | 1.41 | 0.04 | |
| Soil - KS2 | 0.864 | 0.25 | 4 | 1.41 | 0.04 | |
| Soil - KS3 | 0.0864 | 0.25 | 4 | 1.41 | 0.04 | |
| Drains - KD1 | 8640 | 0.25 | 29.4 | 3.281 | 0.04 | |
| Drains - KD2 | 864 | 0.25 | 29.4 | 3.281 | 0.04 | |
| Drains - KD3 | 86.4 | 0.25 | 29.4 | 3.281 | 0.04 | |
| Drains - WL - KD1 | 86400 | 0.7 | 29.4 | 3.281 | 0.04 | |
| Drains - WL - KD2 | 8640 | 0.7 | 29.4 | 3.281 | 0.04 | |
| Drains - WL - KD3 | 864 | 0.7 | 29.4 | 3.281 | 0.04 | |
| Road concrete | 0.0000864 | 0.05 | 1.581 | 1.416 | 0.04 | |
| Road basement | 0.00864 | 0.25 | 4 | 1.416 | 0.04 | |

| Surface flow properties | | | | | |
|-------------------------|---------------------|---------------------------------|-----------------------|---------------------|--------------------|
| | Coupling length | Manning's roughness coefficient | | Rill storage height | Obstruction height |
| Units | l_c [m] | n_x [$m^{-1/3}s$] | n_y [$m^{-1/3}s$] | D_t [m] | O_t [m] |
| Soil | $1. \times 10^{-2}$ | 0.03 | 0.03 | 0.005 | 0.005 |
| Road | $1. \times 10^{-2}$ | 0.018 | 0.018 | 0.001 | 0.001 |

224 In order to simulate each parameter combination, a total of 90 models were developed (27 models for
 225 each road structures and 9 models for natural conditions). Models are run for 10'000 days (about 27 years) with
 226 a constant flux equal to 380mm/y on the top representing the rainfall to reach a steady state. This precipitation
 227 allows for the saturation of the downslope part of the model. Subsequently, subsurface flow rates in the soil layer
 228 were extracted at each section with an area of $0.4m^2$ (1m wide times the soil thickness) presented in Figure 6.
 229 Flow-rates at any given location represent the cumulative vertical flow. Their spatial assessment allows to assess
 230 to what extent the roads perturb the system, and further allows to assess the erosion risk associated with the
 231 induced preferential flow. Therefore, a comparison of flow rates between each model was made to present the
 232 effect of each road structure and sloping fen properties on the dynamics.



233

234 **Figure 6 : Location of observation sections in the models.**

235 3 Results and Discussion

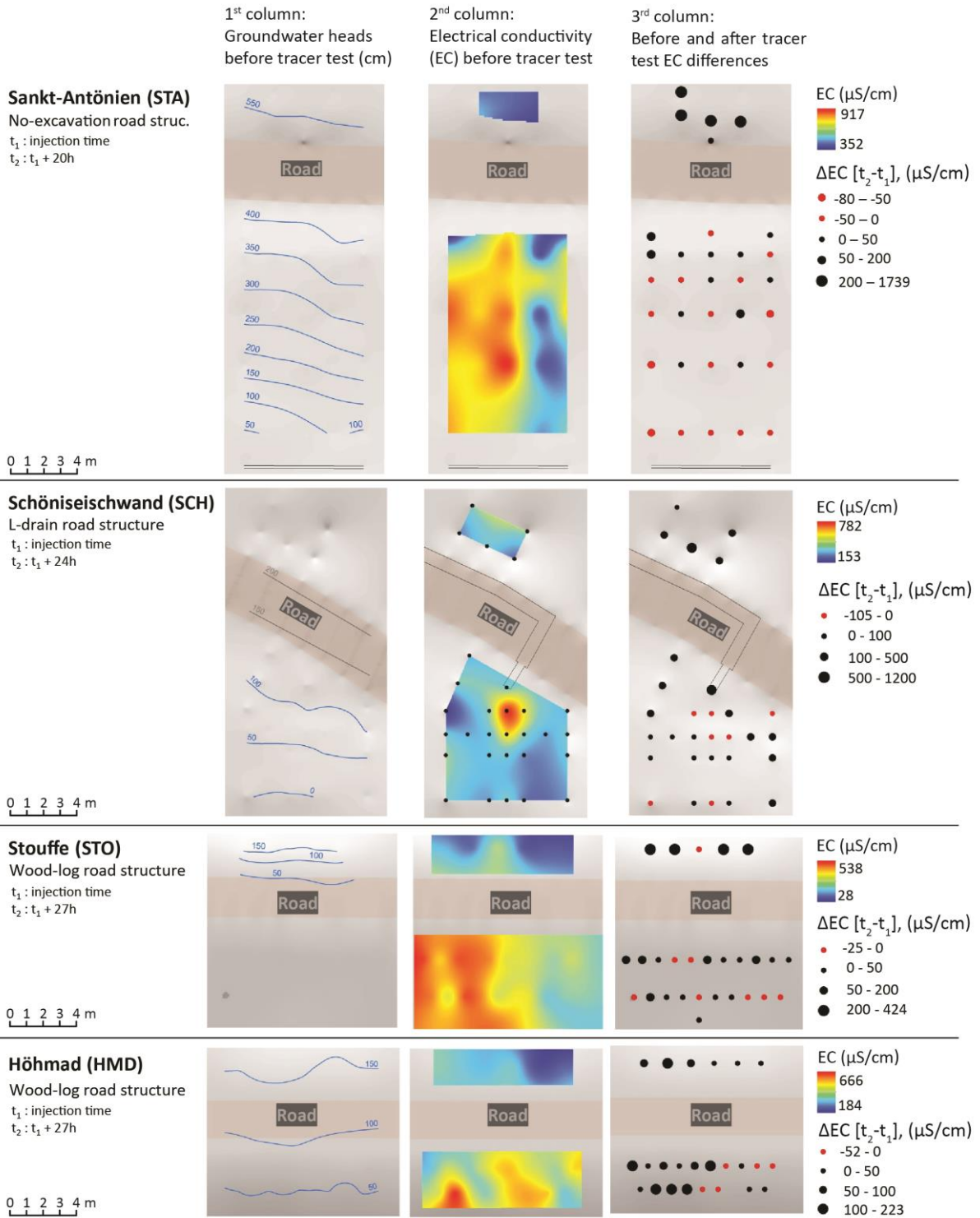
236 3.1 Fieldwork

237 Based on the observations, all sites show a continuous saturated zone before the experiment, both upstream and
 238 downstream of the road, the hydraulic gradients being similar to the terrain slope (Figure 7, 1st column). In
 239 contrast, the EC maps established prior to the tracer test show a spatial variability of one to several meters
 240 (Figure 7, 2nd column.). Within each plot, EC varies from 482 to 629 μ S/cm. At the SCH site, the highest values

241 are located downstream of the L-drain outlet which could indicate that the EC increases as water is flowing
242 through the drain (e.g. through the dissolution of the construction material). Given that this initial distribution of
243 EC is not uniform, the comparison of EC after the sprinkling experiment has to be made in a relative manner
244 (Figure 7, 3rd column).

245 The heterogeneity of the hydraulic conductivity of the soil is apparent from the tracer tests (Figure 7, 3rd
246 column: EC 24 hours after injection). At all four sites, the front of the saline solution is not uniform but follows
247 the heterogeneity of the soil hydraulic conductivity. Nevertheless, road structures may create preferential flow
248 path that is particularly obvious at the SCH site where the front follows two preferential flow paths. One related
249 to the L-drain (right path) and the other on the left, unrelated to the L-drain, suggesting that the latter drains only
250 a part of the water and the other part follows a natural preferential flow path. At the HMD site, the saline
251 solution is far more concentrated on the left side of the plot, yet apparently not as a result of the road's structure.
252 Rather, the soil appears more permeable on the left side of the plot, both upslope and downslope of the road.
253 Finally, the decrease in EC observed 24 hours after injection at some locations might result from the following:
254 (1) the tracer injection induces, by "piston effect", the displacement of a small volume of local water with a
255 lower EC; (2) the tracer injection was preceded by a period of irrigation without tracer, which could have diluted
256 the pre-irrigation soil solution.

257 In each case, the irrigation experiments demonstrate the continuity of subsurface flow under the road for
258 all structures. For the no-excavation and wood-log type, the perturbation of the flow field seems to be controlled
259 by the natural heterogeneity of the soil and flow paths, and not by the road itself. Conversely, the field data
260 strongly suggest that the L-drain constitutes an important preferential pathway and consequently subsurface flow
261 is increasingly concentrated. In terms of wetland conservation, this flow convergence is a serious threat (gully
262 erosion, local drying up of the soil). Despite these strong indications, it is clear that with the field data alone no
263 conclusive analysis can be made as no data before the construction of the road are available. Fieldwork allows
264 for site-specific conclusions, but more general conclusions which are not specific to a site are impossible.
265 Therefore, numerical modelling was used to fill this gap.



266

267 **Figure 7 : Fieldwork results at the four field sites: 1st column) Spline interpolated measured groundwater heads**
 268 **before tracer test , 2nd column) Measured EC before tracer test and 3rd before and after tracer test differences in EC.**

269

270

271 3.2 Modelling

272 Figure 8a shows the results of the models with a slope of 10%, Figure 8b with a slope of 20% and Figure
273 8b with a slope of 30%. In each dot chart, the groundwater flow rates (always in m^3/d) are plotted with crosses
274 for the base case model, diamonds for the no-excavation type, squares for the L-drain type and circles for the
275 wood-log type. In addition, the maximum flow rate capacity of the soil calculated with the Darcy Law (1) and
276 the flow rate induced by the precipitation are also presented for the interpretation of the results. In following
277 paragraphs, the base case (natural conditions) results are presented and discussed, followed by the simulations of
278 the road structures.

279 In the base case model, groundwater flow rates vary from $0.003 \text{ (m}^3/\text{d)}$ to $0.069 \text{ (m}^3/\text{d)}$ for 10% slope,
280 $0.006 \text{ (m}^3/\text{d)}$ to $0.069 \text{ (m}^3/\text{d)}$ for 20% slope and to $0.009 \text{ (m}^3/\text{d)}$ to $0.069 \text{ (m}^3/\text{d)}$ for 30% slope. The groundwater
281 flow rate decreases gradually depending on the hydraulic conductivities (KS) of the soil layer. For any slope,
282 where hydraulic conductivities are high (KS1), groundwater flow rates are higher compared to the case where
283 hydraulic conductivities are low (KS3). The primary observation is that groundwater flow rates are mainly
284 controlled by the hydraulic conductivities and therefore the slope plays a minor role. Differences between the
285 maximum and minimum hydraulic conductivity are two orders of magnitude, whereas changes between slopes
286 multiply by two (for a slope of 20%) or three (for a slope of 30%) the groundwater flow. Therefore the
287 groundwater flow is increased by a factor 3 between the model KS3 with a slope of 10% and model KS3 with a
288 slope of 30%. Finally, it can be seen that the maximum flow rate of the soil is reached and lower than
289 precipitation in all cases except if the hydraulic conductivity is high (KS1). This means that for KS2 and KS3
290 models, surface flow occurs and conversely the soil is able to infiltrate the precipitation in KS1 models.

291 In the no-excavation and wood-log type models, the effect of road structures is quite similar. The
292 groundwater flows vary from $0.01 \text{ (m}^3/\text{d)}$ to $0.069 \text{ (m}^3/\text{d)}$ for 10% slope, $0.01 \text{ (m}^3/\text{d)}$ to $0.069 \text{ (m}^3/\text{d)}$ for 20%
293 slope and to $0.010 \text{ (m}^3/\text{d)}$ to $0.069 \text{ (m}^3/\text{d)}$ for 30% slope. Compared to the base case model, results show that the
294 no-excavation and wood-log type structures have a minimal impact. The only marked difference is that
295 groundwater flow rates are slightly higher if the soil hydraulic conductivities are low (KS3) for each slope in the
296 wood-log type model. This can, to a certain extent, be explained by the fact that the hydraulic conductivity of the
297 base of the road (consisting of wood-logs) is higher than the hydraulic conductivity of the soil and therefore
298 facilitate the infiltration. Conversely, in the base case model, less water is infiltrated but more runoff occurs.
299 However, the process is limited, because at 3.5 m downstream the road ($x=67\text{m}$), the simulated flow rates of the

300 model KS3- KD1 and a slope of 20% for the wood-log and no-road model are equal (Figure 9). For the no-
301 excavation model with a slope of 10%, results are not presented for technical reasons. For this specific geometry
302 and topography, a different structure of the mesh had to be generated which did not allow for a direct visual
303 comparison with the other models. In the 20% and 30% slope models, the results of the no-excavation model are
304 similar to the base case model.

305 In the L-drain type model, the effect is markedly different from the other road structures. The
306 groundwater flows vary significantly in the observation sections. The maximum flows are always obtained in the
307 observation section G just downstream the drain outlet and can be 10 times higher than in the base case.
308 Conversely, minimum flows are obtained in C and D observation sections in which flow rate may be 10 times
309 lower. Significant differences in groundwater flow are also observed in the same transect (i.e. the transect
310 formed by the observation section A, B, C, D, E, F, G and H within the same model). The maximum differences
311 are observed if the hydraulic conductivity of soil (KS) and drain (KD) are high and may vary from 0.025 (m³/d)
312 to 0.150 (m³/d). Conversely, when KS and/or KD are low, the differences along the transect are smaller. The L-
313 drain structures also facilitate water infiltration in soil with a low permeability (KS3) where groundwater flow
314 rates are slightly higher than the base case model. Finally, it can be seen that slope accentuates groundwater flow
315 rate differences along the transect. Therefore, an increase of groundwater flow differences in the same model is
316 observed for the 10% and 30% slope scenarios. The impact of L-drain may be further explored by extracting
317 groundwater flows lower than 3.5m to assess the extent of perturbations. Figure 10 shows additional simulated
318 groundwater flows for the most critical cases (i.e. KS1 with a slope of 10%, 20% and 30%) downstream the road
319 at 3.5m and 6.5m respectively and 2.5m upstream. It can be seen that at 3.5m the groundwater flows already
320 regain their upstream conditions. At 6.5m downstream the road, all observation sections are very close the
321 upstream flows except in section G where flows are still slightly higher.

322 The model results can be used to predict the risk of gully erosion and. Gully erosion may occur when
323 changes in surface flow dynamics induce runoff concentration (Nyssen et al., 2002;Valentin et al., 2005b). As
324 presented in Figure 8, the maximum flow rate capacity of the soil is small in caparison with precipitation. For all
325 model scenarios except for KS1, the soil capacity is lower than the precipitation amount which is already set
326 pretty low in the model. This means that runoff already occurs in sloping fens. However, the runoff may be
327 accentuated by subsurface perturbation caused by the L-drain structures. To illustrate this process, the simulated
328 surface flow velocities of each road structure downstream the road for the model KS2-KD2 and slope of 20% are

329 presented in Figure 11. In this case, maximum flow rate capacity of the soil is approximately equal to
330 precipitation, therefore runoff should not occur. However, it can be seen some runoff in the L-drain model which
331 is the consequence of the subsurface flow concentration. In this configuration, the soil infiltration capacity is too
332 small and consequently, the groundwater emerges and flows on the surface. Although the formation of gullies
333 depends a lot of other factors (Valentin et al., 2005b), such as soil type or the rain intensity, the model showed
334 that downstream L-drain structure may cause runoff concentration which is an important factor. A simple
335 recommendation can be made to avoid this runoff concentration.

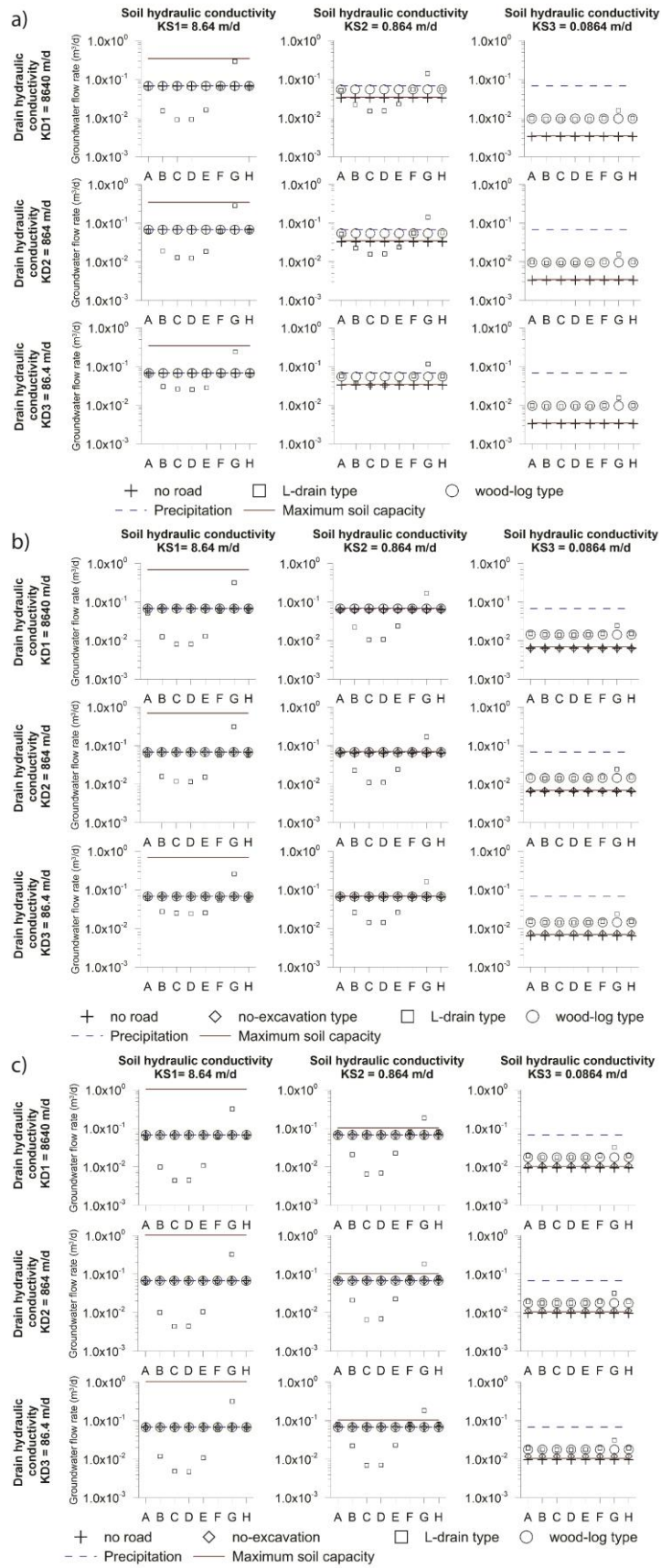
- 336 1. If the maximum flow rate capacity of the soil is smaller than the flow rate induced by precipitation,
337 the installation of an L-drain structure should not be considered.
- 338 2. If the maximum flow rate capacity of the soil is larger than the flow rate induced by precipitation, an
339 L-drain may be considered only if the concentrated flow calculated by multiplying the drainage area
340 by the precipitation is smaller than maximum flow rate capacity of the soil

341 Finally, the impact of road structure on the upstream road dynamics may be also assessed. Figure 12 shows the
342 same information as Figure 8 but at 2.5m upstream. It can be seen that for all models, upstream flows are similar
343 to the base case model. This means that all structures allow the groundwater to flow across the road.

344 The impact of the L-drain road structure which concentrates groundwater flow is clearly identified in the
345 numerical approach and is consistent with the field observations. For other road structures also, numerical
346 models are consistent with fieldwork results by showing relatively undisturbed groundwater flow downslope the
347 road. The development of models with various combinations of parameters also allowed for exploring a larger
348 parameter space than using field work only. For instance, the fact that the impact of an L-drain structure on the
349 water dynamics is less marked if the hydraulic conductivity of soil is low would have been impossible to identify
350 by using fieldwork only. However, a numerical model is always a simplified reproduction of reality. The main
351 model assumption is that hydraulic conductivity of the soil is homogeneous. Groundwater flow in fens can occur
352 along preferential pathways. Therefore, the models are not able to reproduce small-scale observations, i.e. the
353 exact hydraulic head in an individual mini-piezometer. Models results have to be interpreted as an average across
354 multiple preferential flow paths.

355 Further investigations should be carried out to identify groundwater flow threshold values above which a risk of
356 for instance gully erosion is present. This is especially important for L-drain structures where the increase of

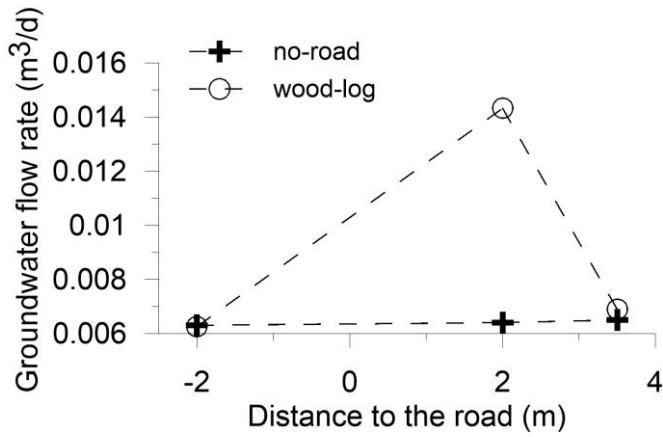
357 flow is higher than for the other structures. Finally, the impact on sloping fen vegetation related to perturbations
358 of the groundwater flow should be further investigated. In this way, road construction could be better planned.



359

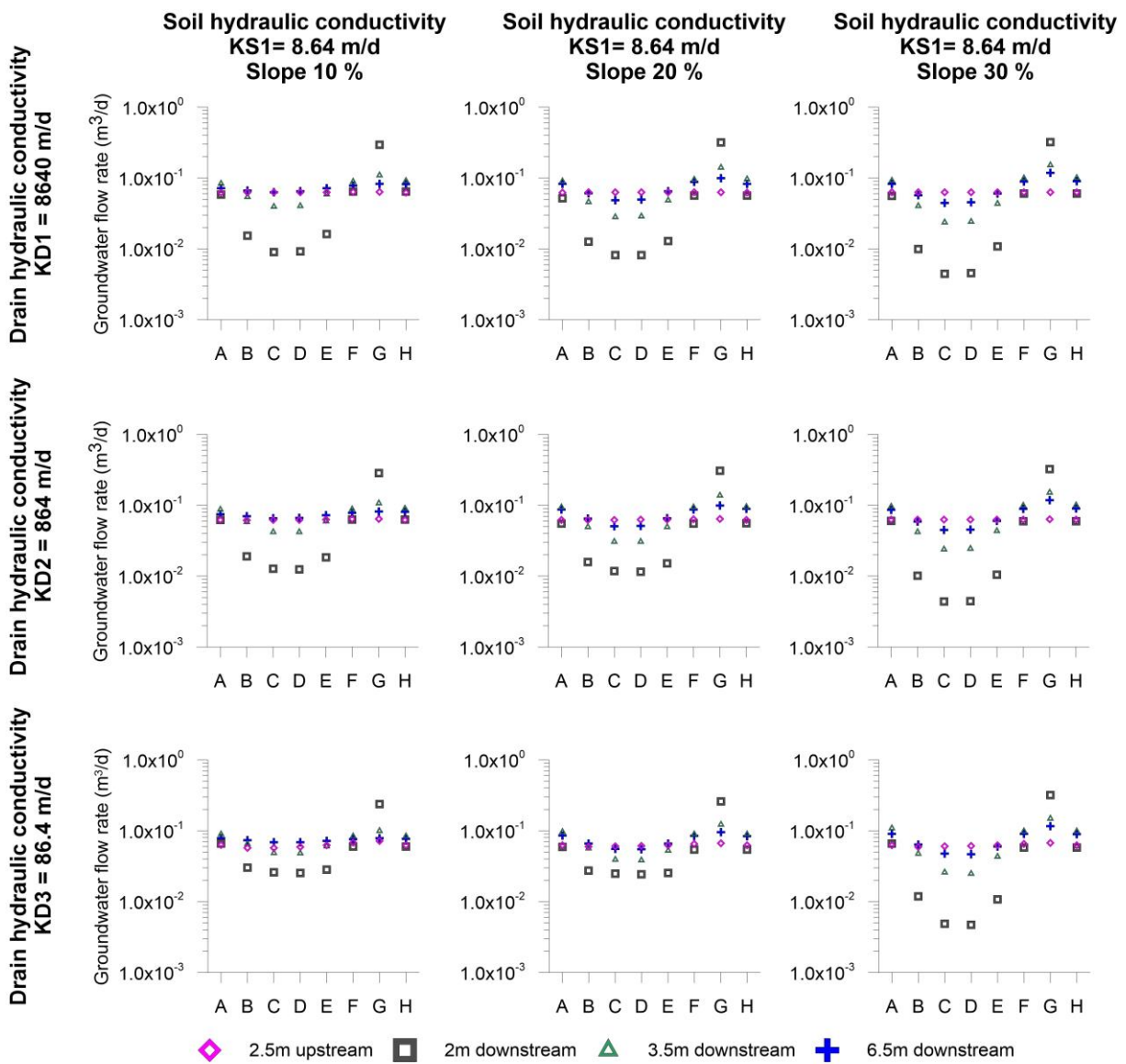
360
361

Figure 8 : Simulated groundwater flow rates 2m downstream each road structures and each parameter combination with a slope of a) 10%, b) 20% and c) 30%.



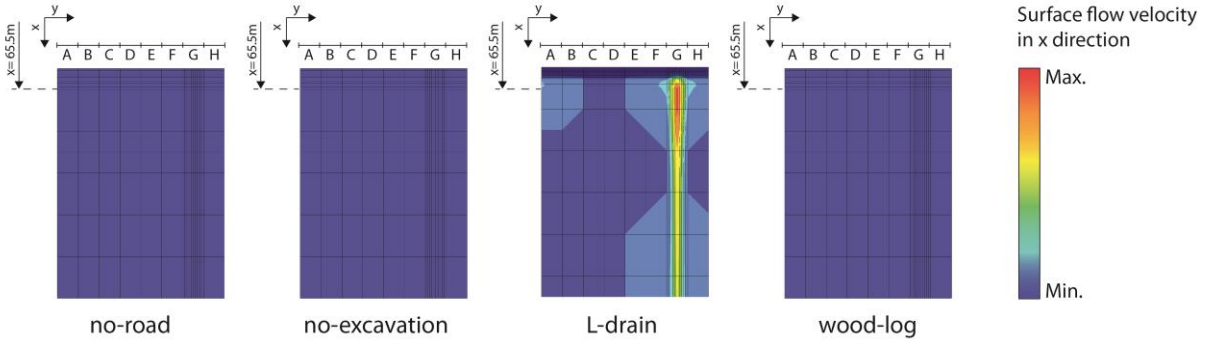
362

363 **Figure 9 : Simulated groundwater flow rates along x direction for the KS3-KD1 models with the wood-log structure**
 364 **and without road.**



365

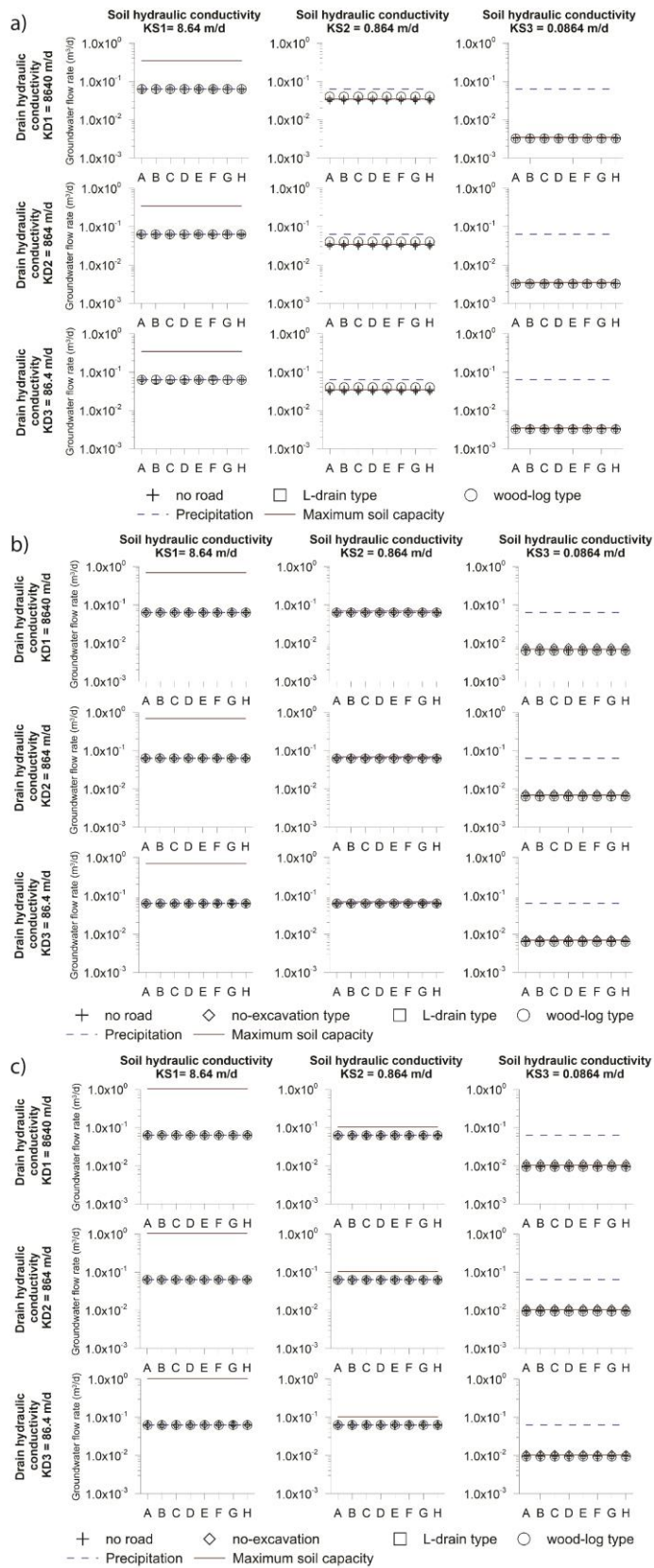
366 **Figure 10 : Extent of perturbations due to the l-drain road type: Simulated groundwater v flow rates at G section at**
 367 **different distances the road.**



368

369

Figure 11 : Simulated surface flow of the KS2-KD2 model and a slope of 20% for each road structure



370

371 **Figure 12 : Simulated groundwater flow rates 2.5m upstream each road structures and each parameter combination**
 372 **with a slope of a) 10%, b) 20% and c) 30%.**

373 **4 Conclusions**

374 This study assessed three road structures regarding their perturbations of the natural groundwater flow.
375 Two of these road structures were specifically developed to reduce the negative impacts of the road. The study is
376 based on two complementary approaches; field-based tracer tests and numerical models simulating groundwater
377 flow for the different road structures.

378 It is the first time that the performance of these road-structures has been investigated in the field. The
379 tracer tests showed that both sides of the road were hydraulically connected for all investigated road structures.
380 Groundwater flow was heterogeneous suggesting the occurrence of preferential flow paths in the soil. The
381 presence of a transversal drain (L-drain) beneath the road constitutes a preferential flow path, however, which is
382 of much greater importance than the naturally occurring preferential pathways. This was also confirmed by the
383 models. Groundwater flow rates 10 times larger than in the natural case were obtained in the numerical
384 simulations. This is not further astonishing as the drains were specifically designed for this purpose. The two
385 other road structures (wood-log and no-excavation) do not perturb the flow field to the extent of the L-drain. To
386 minimize the perturbation of flow fields, the wood-log and no-excavation structures are recommended.

387 The combination of fieldwork and the development of numerical models was fundamental to achieve the
388 goal of this study. The tracer test allowed for a better understanding of groundwater flow throughout road
389 structures and allowed for evaluating their effectiveness at a given location. However, the tracer tests are time-
390 consuming and only a few field sites are available. The numerical approach, on the other hand, allows for
391 exploring any combination of slope, hydraulic properties or road structure, thus providing a more comprehensive
392 approach. In our study, the trends between the numerical and field approaches were consistent.

393 **5 Acknowledgements**

394 This research was funded by the Swiss Federal Office for the Environment (FOEN) and supported by
395 Swiss Federal Office for Agriculture (FOAG). The authors are grateful to Benoit Magnin, Peter Staubli, Andreas
396 Stalder, Anton Stübi and Ueli Salvisberger for their collaborations. We thank the three anonymous reviewers and
397 the editor for their constructive comments.

398 **6 References**

399 Aquanty: HydroGeoSphere, a three-dimensional numerical model describing fully- integrated
400 subsurface and surface flow and solute transport. Waterloo, ON, Canada., 2017.

401 Baker, C., Thompson, J. R. and Simpson, M.: 6. Hydrological Dynamics I: Surface Waters, Flood and
402 Sediment Dynamics The Wetlands Handbook, 1st edition. Edited by E. Maltby and T. Barker. 2009.
403 Blackwell Publishing, 120-168, 2009.

404 Betts, H. D., and DeRose, R. C.: Digital elevation models as a tool for monitoring and measuring gully
405 erosion, *International Journal of Applied Earth Observation and Geoinformation*, 1, 91-101,
406 [http://dx.doi.org/10.1016/S0303-2434\(99\)85002-8](http://dx.doi.org/10.1016/S0303-2434(99)85002-8), 1999.

407 Broggi, M. E.: Minimum requis de surfaces proches de l'état naturel dans le paysage rural, illustré par
408 l'exemple du Plateau suisse. Liebefeld-Berne., Rapport 31a du Programme national de recherche
409 "Sol", 199p, 1990.

410 Brunner, P., and Simmons, C. T.: HydroGeoSphere: a fully integrated, physically based hydrological
411 model, *Groundwater*, 50, 170-176, 2012.

412 Capra, A., Porto, P., and Scicolone, B.: Relationships between rainfall characteristics and ephemeral
413 gully erosion in a cultivated catchment in Sicily (Italy), *Soil and Tillage Research*, 105, 77-87,
414 <http://dx.doi.org/10.1016/j.still.2009.05.009>, 2009.

415 Charman, D.: Peatlands and environmental change. John Wiley & Sons Ltd. 301 2002.

416 Chimner, R. A., Cooper, D. J., Wurster, F. C. and Rochefort, L.: An overview of peatland restoration in
417 North America: where are we after 25 years?, *Restoration Ecology*, 25, 283-292, 2016.

418 Cochand, F., Therrien, R., and Lemieux, J.-M.: Integrated Hydrological Modeling of Climate Change
419 Impacts in a Snow-Influenced Catchment, *Groundwater*, 57, 3-20, doi:10.1111/gwat.12848, 2019.

420 Cognard Plancq, A. L., Bogner, C., Marc, V., Lavabre, J., Martin, C., and Didon Lescot, J. F.: Etude du
421 rôle hydrologique d'une tourbière de montagne: modélisation comparée de couples "averse-crue"
422 sur deux bassins versants du Mont-Lozère., *Etudes de géographie physique*, n° XXXI, p. 3 - 15, 2004.

423 Daba, S., Rieger, W., and Strauss, P.: Assessment of gully erosion in eastern Ethiopia using
424 photogrammetric techniques, *CATENA*, 50, 273-291, [http://dx.doi.org/10.1016/S0341-8162\(02\)00135-2](http://dx.doi.org/10.1016/S0341-8162(02)00135-2), 2003.

426 Derose, R. C., Gomez, B., Marden, M., and Trustrum, N. A.: Gully erosion in Mangatu Forest, New
427 Zealand, estimated from digital elevation models, *Earth Surface Processes and Landforms*, 23, 1045-
428 1053, doi:10.1002/(SICI)1096-9837(1998110)23:11<1045::AID-ESP920>3.0.CO;2-T, 1998.

429 Descroix, L., González Barrios, J. L., Viramontes, D., Poulenard, J., Anaya, E., Esteves, M., and Estrada,
430 J.: Gully and sheet erosion on subtropical mountain slopes: Their respective roles and the scale
431 effect, *CATENA*, 72, 325-339, <http://dx.doi.org/10.1016/j.catena.2007.07.003>, 2008.

432 Dutton, A. L., Loague, K., and Wemple, B. C.: Simulated effect of a forest road on near-surface
433 hydrologic response and slope stability, *Earth Surface Processes and Landforms*, 30, 325-338,
434 10.1002/esp.1144, 2005.

435 Li, Q., Unger, A. J. A., Sudicky, E. A., Kassenaar, D., Wexler, E. J., and Shikaze, S.: Simulating the multi-
436 seasonal response of a large-scale watershed with a 3D physically-based hydrologic model, *Journal of
437 Hydrology*, 357, 317-336, <http://dx.doi.org/10.1016/j.jhydrol.2008.05.024>, 2008.

438 Limpens, J., Berendse, F., Blodau, C., Canadell, J. G., Freeman, C., Holden, J., Roulet, N., Rydin, H. and
439 Schaepman-Strub, G.: Peatlands and the carbon cycle: from local processes to global implications – a
440 synthesis, *Biogeosciences*, 5, 1475-1491, 2008.

441 Lindsay, R.: Peatbogs and carbon: a critical synthesis to inform policy development in oceanic peat
442 bog conservation and restoration in the context of climate change, University of East London,
443 Technical Report, 2010.

444 Loague, K., and VanderKwaak, J. E.: Simulating hydrological response for the R-5 catchment:
445 comparison of two models and the impact of the roads, *Hydrological Processes*, 16, 1015-1032,
446 10.1002/hyp.316, 2002.

447 Martínez-Casasnovas, J. A.: A spatial information technology approach for the mapping and
448 quantification of gully erosion, *CATENA*, 50, 293-308, [http://dx.doi.org/10.1016/S0341-](http://dx.doi.org/10.1016/S0341-8162(02)00134-0)
449 [8162\(02\)00134-0](http://dx.doi.org/10.1016/S0341-8162(02)00134-0), 2003.

450 Nyssen, J., Poesen, J., Moeyersons, J., Luyten, E., Veyret-Picot, M., Deckers, J., Haile, M., and Govers,
451 G.: Impact of road building on gully erosion risk: a case study from the Northern Ethiopian Highlands,
452 *Earth Surface Processes and Landforms*, 27, 1267-1283, 10.1002/esp.404, 2002.

453 Poesen, J., Nachtergaele, J., Verstraeten, G., and Valentin, C.: Gully erosion and environmental
454 change: importance and research needs, *CATENA*, 50, 91-133, [http://dx.doi.org/10.1016/S0341-](http://dx.doi.org/10.1016/S0341-8162(02)00143-1)
455 [8162\(02\)00143-1](http://dx.doi.org/10.1016/S0341-8162(02)00143-1), 2003.

456 Reckendorfer, W., Funk, A., Gschöpf, C., Hein, T. and Schiemer, F.: Aquatic ecosystem functions of an
457 isolated floodplain and their implications for flood retention and management, *Journal of Applied*
458 *Ecology*, 50, 119–128, 2013.

459 Reid, L. M., and Dunne, T.: Sediment production from forest road surfaces, *Water Resources*
460 *Research*, 20, 1753-1761, 10.1029/WR020i011p01753, 1984.

461 Rydin, H. a. J., J.: The biology of peatlands, Oxford University Press, 343p., 2005.

462 Samaritani, E., Siegenthaler, A., Yli-Petäys, M., Buttler, A., Christin, P.-A., and Mitchell, E. A. D.:
463 Seasonal Net Ecosystem Carbon Exchange of a Regenerating Cutaway Bog: How Long Does it Take to
464 Restore the C-Sequestration Function?, *Restoration Ecology*, 19, 480-489, 10.1111/j.1526-
465 100X.2010.00662.x, 2011.

466 Valentin, C., Poesen, J., and Li, Y.: Gully erosion: Impacts, factors and control, *CATENA*, 63, 132-153,
467 <http://dx.doi.org/10.1016/j.catena.2005.06.001>, 2005a.

468 Valentin, C., Poesen, J., and Li, Y.: Gully erosion: Impacts, factors and control, *CATENA*, 63, 132-153,
469 <https://doi.org/10.1016/j.catena.2005.06.001>, 2005b.

470 Van Genuchten, M. T.: A closed-form equation for predicting the hydraulic conductivity of
471 unsaturated soils, *Soil science society of America journal*, 44, 892-898, 1980.

472 VanderKwaak, J. E.: Numerical simulation of flow and chemical transport in integrated surface-
473 subsurface hydrologic systems, Ph.D. thesis, Departement of Earth Science, University of Waterloo,
474 Waterloo, Ontario, Canada., 1999.

- 475 von Sengbusch, P.: Enhanced sensitivity of a mountain bog to climate change as a delayed effect of
476 road construction, *Mires and Peat*, 15: Art. 6, (Online: <http://www.mires-and-peat.net/pages/volumes/map15/map1506.php>), 2015.
- 478 Wemple, B. C., and Jones, J. A.: Runoff production on forest roads in a steep, mountain catchment,
479 *Water Resources Research*, 39, 2003.
- 480 Zollner, A.: Das Abflussgeschehen von unterschiedlich genutzten Hochmooreinzugsgebieten - Bayer.
481 Akad. f. Naturschutz u. Landschaftspflege - Laufen / Salzach, *Laufener Seminarbeitr.* , 111-119, 2003.